

number of electron pairs for that shell (the valence shell capacity, VSC) then the shell is considered to be filled and cannot accept electron density from fluorine atoms to relieve lone-pair-lone-pair repulsions. Instead repulsions between the lone pairs on the central atom and the fluorine lone pairs will produce long bonds. Thus, the observed bond length in  $\text{PF}_3$  (157 pm) in which the valence shell of phosphorus (VSC = 6) has three bonding pairs and one lone pair (total occupancy number,  $\sum\text{ON} = 5$ , <6) is shorter than the calculated value ( $110 + 54 = 165$  pm) because the fluorine lone pairs can delocalize into the incomplete valence shell of phosphorus. In contrast in  $\text{SF}_2$  ( $\sum\text{ON} = 6$ ) the bond length of 159 pm is close to the calculated value of  $104 + 54 = 158$  pm. Similarly in  $\text{BrF}_2^+$  ( $\sum\text{ON} = 6$ ) the bonds are of normal length (169 pm), while in  $\text{BrF}$  ( $\sum\text{ON} = 7$ , >6) the bond is long (176 pm), as are the basal bonds (177 pm) in  $\text{BrF}_5$  ( $\sum\text{ON} = 7$ ). In  $\text{BrF}_4^-$  ( $\sum\text{ON} = 8$ ) the bonds are still longer (181 pm). Examples are shown in Table IV.

### Conclusions

A covalent radius for fluorine of 54 pm gives calculated bond lengths in agreement with experiment for those species in which the bonds are expected to be "normal", that is, in which the central atom has a filled valence shell and no lone pairs. In species in which the central atom has an incomplete valence shell, electron delocalization from fluorine gives short bonds. In species in which there are lone pairs in a filled valence shell on the central atom, lone-pair repulsions give long bonds. In species in which there are lone pairs in an incomplete valence shell, an empirical rule for the effective size of the domain of a lone pair enables us to decide if the capacity of the valence shell is, or is not, exceeded and, therefore, if the bonds are expected to be long, normal, or short.

Contribution from the Departments of Chemistry, University of Michigan, Ann Arbor, Michigan 48109, and Universitat Autònoma de Barcelona, Bellaterra, 08193 Barcelona, Spain

### A Dinuclear Vanadyl(IV) Complex of 3,5-Dicarboxypyrazole: Synthesis, Crystal Structure, and Electron Spin Resonance Spectra

Carl W. Hahn,<sup>†</sup> Paul G. Rasmussen,<sup>\*†</sup> and J. Carlos Bayón<sup>†</sup>

Received July 24, 1991

### Introduction

Our previous work with 3,5-dicarboxypyrazole ( $\text{H}_3\text{Dcp}$ ) as a dinucleating ligand has shown that the ligand readily accommodates a number of transition metals ions in square-planar configuration.<sup>1</sup> This report shows that the ligand will also bind  $\text{VO}^{2+}$  in a dinuclear fashion. The only metal previously reported to chelate with Dcp, which possesses unpaired electrons, is copper. The copper centers, whose unpaired electrons lie in the  $d_{x^2-y^2}$  orbital, were found to couple antiferromagnetically ( $2J = -200.2$   $\text{cm}^{-1}$ ) via superexchange through the pyrazole bridge. The vanadyl ion similarly has a single unpaired electron. However, the electronic coupling of the vanadyl ions is through the  $d_{xy}$  orbital in the ground state.

There has been some previous work on vanadyl dimers and their electronic interactions.<sup>2</sup> These dimers show a tendency toward spin exchange when their orbitals are able to interact. Direct  $d_{xy}$ - $d_{xy}$  overlap generally results in antiferromagnetic coupling. Their tendency toward superexchange is limited, as the ground-

Table I. Crystal Data and Structure Determination Summary

compd	$(\text{Bu}_4\text{N})_2[(\text{VO})_2(\text{Dcp})_2]$
empirical formula	$\text{C}_{42}\text{H}_{74}\text{N}_6\text{O}_{10}\text{V}_2$
fw	924.97 <sub>5</sub>
cryst color and habit	purple prisms
cryst dimens	$0.15 \times 0.12 \times 0.06$ mm <sup>3</sup>
cryst system	triclinic
space group	$P\bar{1}$ (No. 2)
Z	2
a	12.809 (6) Å
b	12.515 (8) Å
c	18.050 (8) Å
$\alpha$	81.32 (4)°
$\beta$	91.16 (4)°
$\gamma$	118.13 (4)°
V	2518 (2) Å <sup>3</sup>
d(calc)	1.220 g cm <sup>-3</sup>
F(000)	9.98 electrons
linear abs coeff ( $\mu$ )	4.1 cm <sup>-1</sup>
radiation type	Mo K $\alpha$ , $\lambda = 0.71073$ Å, Lp corrected, graphite monochromator
temp	ambient
$R^a$	0.0837
$R_w^b$	0.0640

$$^a R = \sum(|F_o| - |F_c|) / \sum|F_o| \quad ^b R_w = [\sum(|F_o| - |F_c|)^2 / \sum w|F_o|^2]^{1/2}$$

state unpaired electron typically lies in the  $d_{xy}$  orbital in a vanadyl complex of  $C_{4v}$  symmetry. However, other mechanisms for exchange exist and several vanadyl dimers have shown weakly coupled exchange to give a low-lying triplet state, as evidenced by ESR spectroscopy.<sup>3</sup>

The best characterized of these triplets are the vanadyl tartrates, most notably the sodium salt of vanadyl(IV) *d,l*-tartrate.<sup>3a</sup> The vanadyl *d,l*-tartrate forms a bis chelate containing two vanadyl ions in an anionic complex, similar to our system. The vanadyl *d,l*-tartrate anion also crystallizes in a roughly coplanar fashion with a metal-metal distance of 4.082 Å.<sup>4</sup> The main difference lies in the lower symmetry of the tartrates and the relative arrangement of the vanadyl oxygen atoms. Relative to the vanadium-vanadium vector, they are trans in the tartrates while they are cis in our complex.

### Experimental Section

$(\text{Bu}_4\text{N})_2[(\text{VO})_2(\text{Dcp})_2]$  was prepared by dissolving 3,5-dicarboxypyrazole hydrate (0.250 g, 1.44 mmol) in 25 mL of hot water. To this was added a solution of vanadyl sulfate hydrate (0.235 g, 1.44 mmol) in 5 mL of water. Addition of a 4.3-mL aliquot of tetrabutylammonium hydroxide (1 M in MeOH) caused the solution to turn purple. Evaporation to dryness and trituration of the residue with *tert*-butyl alcohol followed by filtration gave the purple crystalline complex. Recrystallization is done by dissolving the complex in acetone and layering it with *tert*-butyl alcohol. Yield: 0.4667 g (70%). IR (KBr pellet):  $\nu(\text{COO})$  1681  $\text{cm}^{-1}$ ,  $\nu(\text{VO})$  1012  $\text{cm}^{-1}$ . Anal. Calc for  $\text{C}_{42}\text{H}_{74}\text{N}_6\text{O}_{10}\text{V}_2$ : C, 54.54; H, 8.06; N, 9.09. Found: C, 54.77; H, 7.91; N, 8.97. Mp: 256–258 °C.

**Physical Measurements.** UV-visible spectroscopy was performed on a Shimadzu UV-160 spectrophotometer. Cyclic voltammetry was performed on a Princeton Applied Research (PAR) potentiostat/galvanostat, Model 173, a PAR universal programmer, Model 175, and a PAR digital coulometer, Model 179. Working and reference electrodes were platinum wire with a silver wire counter electrode. ESR spectroscopy was performed on a Bruker ER 200E-SRC spectrometer equipped with a low-temperature cavity and controller. X-ray diffraction data were gathered on a Syntex P2, diffractometer. The structure solutions were routine with procedures previously described.<sup>5</sup> The parameters used

- Bayón, J. C.; Esteban, P.; Net, G.; Rasmussen, P. G.; Baker, K. N.; Hahn, C. W.; Gumz, M. M. *Inorg. Chem.* 1991, 30, 2572.
- Syamal, A. *Coord. Chem. Rev.* 1975, 16, 309.
- (a) Belford, R. L.; Chasteen, N. D.; So, H.; Tapscott, R. E. *J. Am. Chem. Soc.* 1969, 91, 4675. (b) Tapscott, R. E.; Belford, R. L. *Inorg. Chem.* 1967, 6, 735. (c) Toy, A. D.; Smith, T. D.; Pilbrow, J. R. *Aust. J. Chem.* 1974, 27, 1. (d) McIlwain, M. E.; Tapscott, R. E.; Coleman, W. F. *J. Magn. Reson.* 1977, 26, 35. (e) Thanabal, V.; Krishnan, V. *Inorg. Chem.* 1982, 21, 3606. (f) Boyd, P. D. W.; Smith, T. D. *J. Chem. Soc., Dalton Trans.* 1972, 839.
- Tapscott, R. E.; Belford, R. L.; Paul, I. C. *Inorg. Chem.* 1968, 7, 356.

<sup>†</sup> University of Michigan.

<sup>†</sup> Universitat Autònoma de Barcelona.

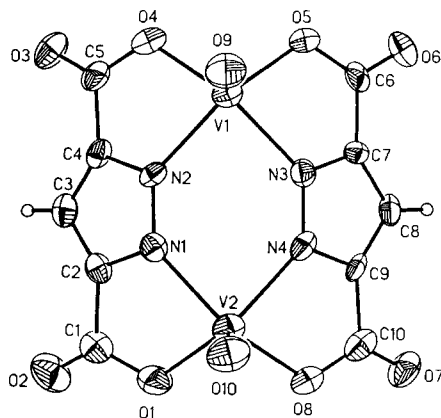


Figure 1. Structure of the  $[(VO)_2(Dcp)_2]^{2-}$  anion.

during X-ray data collection are summarized in Table I and Table S1 (supplementary material).

### Structural Description of the $(VO)_2(Dcp)_2$ Anion

There are no previously reported vanadium dimers containing pyrazole as a bridging ligand. The trianion of the ligand (Dcp) binds two vanadyl ions to form the complex  $(Bu_4N)_2[(VO)_2(Dcp)_2]$ . An ORTEP plot of the anion is shown in Figure 1. The two vanadyl oxygen atoms are cis to one another, and a crystal-packing plot shows no evidence of chain formation along the  $z$  axis although a coordination site remains open. The geometry around both metal atoms is a nearly regular square pyramid with all of the angles between the axial  $V=O$  bond and four equatorial bonds being very nearly  $110^\circ$ . The eight equatorial donor atoms lie in an approximate plane with the metal atoms about  $0.6 \text{ \AA}$  above that plane. However, the two ligands are folded out of the plane to form a sawhorse type structure.

All bond lengths are normal. The  $V-O(\text{carboxylate})$  bonds average  $1.981(7) \text{ \AA}$  and the  $V-O(\text{pyrazole})$  bonds average  $2.032(8) \text{ \AA}$ . The two  $V=O$  bonds are  $1.56$  and  $1.57 \text{ \AA}$ . These are similar to those found for the vanadyl sulfates<sup>6,7</sup> and nearly identical to that of  $VO(\text{acac})_2$ .<sup>8,9</sup> The infrared stretch corresponding to  $\nu(V=O)$  was assigned to an intense peak at  $1012 \text{ cm}^{-1}$ .

The  $V-V$  distance in the compound is  $4.206 \text{ \AA}$ . This small intermetallic distance allows for through-space electronic interactions as well as exchange through the bridging ligand. It is notable that the intermetallic distance for complexes of 3,5-dicarboxypyrazole increases in the order  $Pd(3.89 \text{ \AA}) < Cu(3.99 \text{ \AA}) < VO(4.2 \text{ \AA})$  demonstrating the flexibility of the ligand. Atomic coordinates are given in Table II. Tables of bond lengths and angles are given in the supplementary material (Tables S3 and S4).

### Results and Discussion

Other vanadyl dimers have been found to have low-lying triplet states, as evidenced by ESR spectroscopy. The complex  $(Bu_4N)_2[(VO)_2(Dcp)_2]$  also shows such behavior, with the ESR spectrum showing the metals to be weakly coupled both at room temperature in solution and at liquid nitrogen temperature in a frozen glass. The room-temperature ESR spectrum of  $(Bu_4N)_2[(VO)_2(Dcp)_2]$  in acetone displays a well resolved isotropic spectrum comprising 15 lines. The spectrum, shown in Figure

Table II. Atomic Positional and Thermal Parameters

atom	x	y	z	$U(EQ), \text{ \AA}^2$
V1	0.0874 (2)	0.1593 (2)	0.2927 (1)	0.054 (1)
V2	0.4556 (2)	0.3427 (2)	0.3158 (1)	0.057 (1)
O1	0.5564 (7)	0.2679 (8)	0.3034 (5)	0.080 (3)
O2	0.5616 (8)	0.0909 (9)	0.2993 (5)	0.112 (3)
O3	0.0141 (7)	-0.1814 (7)	0.2589 (5)	0.083 (3)
O4	0.0012 (6)	-0.0133 (7)	0.2732 (4)	0.065 (2)
O5	0.0096 (6)	0.2170 (7)	0.2112 (4)	0.061 (2)
O6	0.0328 (7)	0.3660 (7)	0.1161 (4)	0.072 (3)
O7	0.5785 (7)	0.6377 (8)	0.1508 (5)	0.087 (3)
O8	0.5636 (6)	0.4957 (7)	0.2484 (4)	0.065 (2)
O9	0.0436 (6)	0.1642 (7)	0.3716 (4)	0.077 (3)
O10	0.4583 (7)	0.3719 (7)	0.3977 (4)	0.077 (3)
N1	0.3320 (8)	0.1662 (8)	0.3127 (5)	0.047 (3)
N2	0.2157 (8)	0.1076 (8)	0.3037 (5)	0.042 (3)
N3	0.2214 (8)	0.3264 (8)	0.2495 (5)	0.048 (3)
N4	0.3383 (8)	0.3841 (8)	0.2563 (5)	0.048 (3)
C1	0.510 (1)	0.148 (1)	0.3013 (7)	0.065 (3)
C2	0.375 (1)	0.089 (1)	0.2999 (6)	0.051 (3)
C3	0.285 (1)	-0.019 (1)	0.2837 (6)	0.062 (3)
C4	0.186 (1)	-0.004 (1)	0.2862 (6)	0.046 (3)
C5	0.058 (1)	-0.077 (1)	0.2706 (7)	0.063 (3)
C6	0.075 (1)	0.324 (1)	0.1686 (7)	0.056 (3)
C7	0.200 (1)	0.385 (1)	0.1865 (6)	0.040 (3)
C8	0.303 (1)	0.482 (1)	0.1540 (7)	0.055 (3)
C9	0.389 (1)	0.479 (1)	0.1990 (7)	0.046 (3)
C10	0.521 (1)	0.549 (1)	0.1968 (8)	0.069 (3)
N5	0.8775 (8)	0.5888 (8)	0.1095 (5)	0.047 (3)
C511	0.7956 (9)	0.4794 (9)	0.0722 (6)	0.059 (3)
C512	0.666 (1)	0.435 (1)	0.0899 (7)	0.079 (3)
C513	0.593 (1)	0.310 (1)	0.0628 (8)	0.117 (3)
C514	0.472 (1)	0.262 (1)	0.0785 (9)	0.166 (4)
C521	0.8597 (9)	0.5574 (9)	0.1939 (6)	0.058 (3)
C522	0.873 (1)	0.447 (1)	0.2283 (6)	0.080 (3)
C523	0.863 (1)	0.436 (1)	0.3132 (7)	0.094 (3)
C524	0.875 (1)	0.331 (1)	0.3528 (8)	0.145 (4)
C531	1.0020 (9)	0.620 (1)	0.0828 (6)	0.061 (3)
C532	1.1020 (9)	0.726 (1)	0.1112 (6)	0.070 (3)
C533	1.2179 (9)	0.739 (1)	0.0840 (7)	0.079 (3)
C534	1.325 (1)	0.841 (1)	0.1067 (8)	0.128 (3)
C541	0.8541 (9)	0.6985 (9)	0.0895 (6)	0.051 (3)
C542	0.866 (1)	0.748 (1)	0.0075 (6)	0.070 (3)
C543	0.841 (1)	0.855 (1)	-0.0073 (6)	0.076 (3)
C544	0.853 (1)	0.910 (1)	-0.0893 (7)	0.104 (3)
N6	0.6640 (8)	-0.1822 (8)	0.3714 (5)	0.054 (3)
C611	0.6719 (9)	-0.293 (1)	0.4129 (6)	0.068 (3)
C612	0.795 (1)	-0.278 (1)	0.4177 (7)	0.090 (3)
C613	0.791 (1)	-0.392 (1)	0.4622 (8)	0.110 (3)
C614	0.912 (1)	-0.379 (1)	0.4732 (8)	0.149 (4)
C621	0.536 (1)	-0.208 (1)	0.3798 (7)	0.077 (3)
C622	0.4427 (9)	-0.311 (1)	0.3442 (6)	0.073 (3)
C623	0.320 (1)	-0.323 (1)	0.3624 (8)	0.105 (3)
C624	0.225 (1)	-0.415 (1)	0.3274 (8)	0.145 (4)
C631	0.7034 (9)	-0.1633 (9)	0.2891 (6)	0.058 (3)
C632	0.694 (1)	-0.060 (1)	0.2383 (6)	0.071 (3)
C633	0.739 (1)	-0.052 (1)	0.1593 (6)	0.081 (3)
C634	0.738 (1)	0.053 (1)	0.1053 (7)	0.119 (3)
C641	0.742 (1)	-0.066 (1)	0.4023 (6)	0.066 (3)
C642	0.734 (1)	-0.073 (1)	0.4872 (7)	0.097 (3)
C643	0.781 (1)	0.053 (1)	0.5097 (8)	0.100 (3)
C644	0.686 (1)	0.089 (1)	0.5018 (9)	0.178 (4)

2, was fit by an interactive iterative procedure using Lorentzian line shapes and manual adjustment of line positions. The fitting corresponds closely to that expected for an isotropic exchange of an electron with two equivalent  $^{51}\text{V}(I = 7/2)$  nuclei, giving integrated peak intensity ratios of  $1:2:3:4:5:6:7:8:7:6:5:4:3:2:1$ .

The frozen-glass ESR spectrum is typical of a triplet. The spectrum, shown in Figure 3, shows overlapping low- and high-field parallel and perpendicular transitions in the  $\Delta M_s \pm 1$  region. A weak transition also occurs at  $g \sim 4$  as the result of "forbidden"  $\Delta M_s \pm 2$  triplet-singlet transitions. The values of  $g_{\parallel}$ ,  $A_{\parallel}$ , and  $D$  were measured directly from the spectrum based on these peak assignments. The values of  $g_{\perp}$  and  $A_{\perp}$  were then calculated from the relations

$$g = (g_{\parallel} + 2g_{\perp})/3 \quad A = (A_{\parallel} + 2A_{\perp})/3$$

- (5) Computations were carried out on an Amdahl 5860 computer. Computer programs used during the structural analysis were from the SHELX program package by George Sheldrick, Institut für Anorganische Chemie der Universität Göttingen, Germany. Other programs include ORTEP, by C. K. Johnson, PLUTO, a crystallographic plotting program, and GEOMIN, a geometry calculation program supplied by the Cambridge University Chemical Laboratory, Cambridge, England.
- (6) Dodge, R. P.; Templeton, D. H.; Zalkin, A. *J. Chem. Phys.* **1961**, *35*, 55.
- (7) Hon, P. K.; Belford, R. L.; Pfluger, C. E. *J. Chem. Phys.* **1965**, *43*, 3111.
- (8) Ballhausen, C. J.; Djurinskij, B. F.; Watson, K. J. *J. Am. Chem. Soc.* **1968**, *90*, 3305.
- (9) Tachez, M.; Thöbald, F.; Watson, K. J.; Mercier, R. *Acta Crystallogr., Sect. B* **1979**, *35*, 1545.

Table III. ESR Data for Spin-Coupled Dimeric Vanadyl Complexes

compd	$g_{\parallel}$	$A_{\parallel}$ , $\text{cm}^{-1}$	$g_{\perp}$	$A_{\perp}$ , $\text{cm}^{-1}$	$D$ , $\text{cm}^{-1}$	ref
$(\text{Bu}_4\text{N})_2[(\text{VO})_2(\text{Dcp})_2]$	1.95	0.0074	1.98	0.0038	0.0343	this work
$\text{Na}_4[\text{VO}(d,l\text{-tartrate})]_2 \cdot 12\text{H}_2\text{O}$	1.953	0.00723	1.982	0.00213	0.0334	3a
$\text{Na}_4[\text{VO}(d\text{-tartrate})]_2 \cdot 6\text{H}_2\text{O}$	1.950	0.00732	1.984	0.00246	0.0335	3a
$[\text{VO}(\text{TCP})]_2(\text{K}^+)_4$	1.967	0.007715	1.987	0.002598	0.02685 0.02610	3e

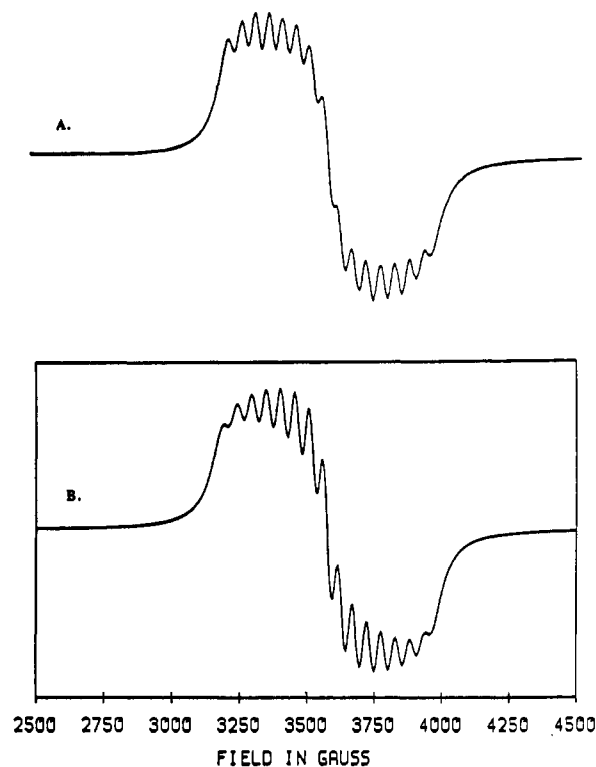


Figure 2. (A) Room-temperature ESR spectrum of  $(\text{Bu}_4\text{N})_2[(\text{VO})_2(\text{Dcp})_2]$  in acetone. (B) Simulated ESR spectrum for  $(\text{Bu}_4\text{N})_2[(\text{VO})_2(\text{Dcp})_2]$  using  $g = 1.97$  and  $A = 50.44 \times 10^{-4} \text{ cm}^{-1}$  (line width = 53 G).

The isotropic  $g$  and  $A$  values are from the isotropic room-temperature spectrum. The resulting parameters are compared with those of related vanadium dimers in Table III.

The point-dipole approximation for an axially symmetric system may be used to confirm the value of the zero-field-splitting parameter.<sup>3a</sup> Using the crystallographically determined V–V distance (4.206 Å) and the  $g$  values gives calculated zero-field values of  $D = 0.0332 \text{ cm}^{-1}$  and  $D = 0.0342 \text{ cm}^{-1}$  for  $g_{\parallel}$  and  $g_{\perp}$ , respectively. These values are in very good agreement with the value of  $D = 0.0343 \text{ cm}^{-1}$  extracted from the spectrum.

The electronic spectrum for  $(\text{Bu}_4\text{N})_2[(\text{VO})_2(\text{Dcp})_2]$  shows the three optical bands expected for a vanadyl complex. The assignments of the bands for the complex follow the Ballhausen and Gray model for the one-electron transitions  $d_{xy} \rightarrow d_{xz}, d_{yz}, d \rightarrow d_{x^2-y^2}$ , and  $d \rightarrow d_{z^2}$ , respectively.<sup>10</sup> The bands occur at 609 nm ( $\epsilon = 8.21 \text{ cm}^{-1}$ ), 530 nm ( $\epsilon = 10.01 \text{ cm}^{-1}$ ), and 431 nm ( $\epsilon = 7.21 \text{ cm}^{-1}$ ), respectively. The energy of the third band shows that the vanadyl remains five-coordinate in solution, as axial coordination of a sixth ligand would cause it to occur at  $<333 \text{ nm}$ .<sup>11</sup> The lower symmetry in the vanadyl  $d,d$ -tartrate spin-triplet dimer lifts the  $d_{xz}, d_{yz}$  degeneracy, giving rise to four optical bands.<sup>3b</sup>

Cyclic voltammetry of  $(\text{Bu}_4\text{N})_2[(\text{VO})_2(\text{Dcp})_2]$  showed two irreversible reduction waves at  $-2.3$  and  $-2.5 \text{ V}$  (vs  $\text{Ag}/\text{AgNO}_3$ ). There is also a broad irreversible oxidation wave at  $+0.85 \text{ V}$  with a shoulder at  $+0.90 \text{ V}$ , suggesting two very closely spaced, irreversible one-electron oxidations.

The treatment of the vanadyl complex with *tert*-butyl hydroperoxide (2:1 metal to peroxide) in dichloromethane resulted in

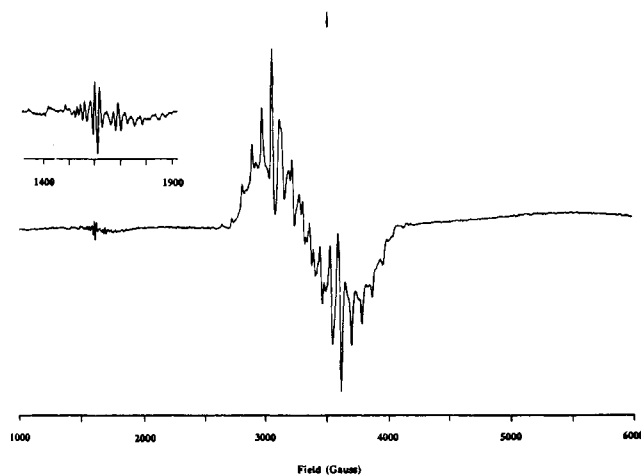


Figure 3. ESR spectrum of the  $(\text{Bu}_4\text{N})_2[(\text{VO})_2(\text{Dcp})_2]$  complex at 93 K in acetone/2-propanol/methanol (15:4:1) glass. Inset shows expanded  $\Delta M_s = \pm 2$  transition.

protonation of the ligand, which precipitated from solution. A similar result was noted for hydrogen peroxide. The complex appears to lose its integrity upon oxidation and does not facilitate the formation of a peroxo adduct.

**Acknowledgment.** P.G.R. acknowledges support from the donors of the Petroleum Research Fund, administered by the American Chemical Society. J.C.B. acknowledges support from the Spanish DGICYT Project PB88-0252. C.W.H. acknowledges support from undergraduate research funds of the College of Literature, Science and the Arts. The assistance of Dr. Jeffrey Kampf, X-ray crystallographer of the Department of Chemistry for data collection, is gratefully acknowledged.

**Supplementary Material Available:** Tables of thermal parameters, bond lengths, bond angles, and crystallographic data (8 pages); a listing of structure factors (24 pages). Ordering information is given on any current masthead page.

Contribution from the Department of Chemistry,  
Tulane University, New Orleans, Louisiana 70118

### Conversion of Chlorofluorocarbons into Chlorofluorohydrocarbons Using the Atherton–Todd Reaction with Dimethyl Phosphonate

Emil Georgiev, D. Max Roundhill,\* and Koljo Troev<sup>1</sup>

Received September 27, 1991

#### Introduction

Chlorofluorocarbons in the stratosphere are environmentally harmful because the photolytic cleavage of their carbon–chlorine bonds results in depletion of the ozone layer.<sup>2</sup> Chlorofluoro-

(10) Ballhausen, C. J.; Gray, H. B. *Inorg. Chem.* 1962, 1, 111.  
(11) Deeth, R. J. *J. Chem. Soc., Dalton Trans.* 1991, 1467.

(1) Permanent address: Central Laboratory for Polymers, Bulgarian Academy of Sciences, Sofia, Bulgaria.  
(2) Molina, M. J.; Rowland, F. S. *Nature* 1974, 249, 810–2. Rowland, F. S. *Am. Sci.* 1989, 77, 36–45.